

The Newtonian Forces in the Kerr Geometry*

Sandip K. Chakrabarti *Tata Institute of Fundamental Research, Homi Bhabha Road, Colaba, Bombay 400005*

A. R. Prasanna *Physical Research Laboratory, Navarangpura, Ahmedabad 380009*

Received 1989 June 12; accepted 1989 October 16

Abstract. We study the properties of the ‘Newtonian forces’ acting on a test particle in the field of the Kerr black hole geometry. We show that the centrifugal force and the Coriolis force reverse signs at several different locations. We point out the possible relevance of such reversals particularly in the study of the stability properties of the compact rotating stars and the accretion discs in hydrostatic equilibria.

Key words: black holes—accretion discs—stability

In spite of the beautiful description of physics through geometry expressed by Einstein’s general relativity seventy-five years ago, and its resurrection during the last twenty-five years, a large percentage of physicists still feel comfortable to discuss the dynamics of a particle in terms of the ‘Newtonian forces’ such as the centrifugal force, Coriolis force *etc.* which are introduced in the early stages of one’s education. Although Einstein’s description of the motion of the particles in a given curved spacetime in terms of their geodesics is very general, understanding the ‘physical significance’ of the various terms that occur in the equation giving the total acceleration is not always possible. However, it has been shown (Abramowicz, Carter & Lasota 1988, hereinafter referred to as ACL) recently that in a conformally projected three-geometry of the four-dimensional manifold where the null lines of the four-geometry are the geodesics, a reference frame exists where the total force acting on a test particle may be split into the gravitational, the centrifugal and the Coriolis terms. This is called the Optical Reference Geometry (ORG).

In this paper we present and analyze these forces in the Kerr geometry, which is the most general solution that represents the spacetime outside a compact rotating object. We show, however, that these forces do not always have the ‘Newtonian’ behaviour.

The frame of reference as expressed in ORG is obtained through the decomposition,

$$ds^2 = \Phi [\tilde{g}_{ik} dx^i dx^k - (dt + 2\alpha_i dx^i)^2] \quad (1)$$

which on comparison with $ds^2 = g_{\alpha\beta} dx^\alpha dx^\beta$ for the Kerr metric yields on the equatorial plane (in Boyer–Lindquist coordinates),

$$\tilde{g}_{rr} = r^3 / [(r-2)\Delta], \quad \tilde{g}_{\phi\phi} = r^2 \Delta / (r-2)^2, \quad \Phi = (1 - 2/r), \quad \Delta = r^2 - 2r + a^2,$$

* Received honourable mention in the 1989 Gravity Research Foundation essay competition.

and

$$\alpha_\phi = a/(r-2). \quad (2)$$

Here, a is the Kerr parameter.

If we now consider a test particle in motion, the forces acting on it as expressed by the ACL equation are given by,

$$m\Phi(f_i - 2\alpha_i f_0) = p^j \tilde{\nabla}_j p_i + 1/2 m^2 \partial_i \Phi + 2E p^j \omega_{ij}, \quad (3)$$

where, $p^i = \Phi p^i$, is the 3-momentum in the projected conformal space (ORG) and $\tilde{\nabla}_j$ is the covariant derivative with respect to the 3-metric \tilde{g}_{ik} . The three terms on the right-hand side may be interpreted as the contributions from the centrifugal force, the gravitational force and the Coriolis force respectively provided a negative sign is taken throughout to match the conventional direction for gravitational force (one identifies the gravitational potential = $-\Phi/2$). With this convention one can see that in Kerr geometry, various quantities take the form

$$\begin{aligned} \omega_{r\phi} &= -a/(r-2)^2, \\ p^\phi &= El(r-r_i)(r-2)/[r^2 \Delta], \\ r_i &= 2(1-a/l). \end{aligned} \quad (4)$$

Here, E and l are the conserved specific energy and the specific angular momentum of the test particle respectively: $E = u_t$ and $l = u_\phi/u_t$, where u_ϕ and u_t are the covariant components of the four velocity and m is the mass of the test particle. In the absence of a better word, we shall call r ‘the p^ϕ reversal radius’ as the sign of p^ϕ changes at this location. In the Schwarzschild geometry ($a = 0$), it is observed (Abramowicz & Prasanna 1989, hereinafter AP) that the centrifugal force (Coriolis force is identically zero) *reverses sign* at the circular photon orbit ($r = 3$) which is the minimum of the proper circumferential radius \tilde{r} of the projected orbit in the ORG defined by,

$$\tilde{r}^2 = \tilde{g}_{ik} \tilde{\delta}^i \tilde{\delta}^k \quad (5)$$

where $\tilde{\delta}^i$ is the azimuthal (spacelike) Killing vector satisfying the Killing equation, $\tilde{\nabla}_{(i} \tilde{\delta}_{j)}$

As this quantity is independent of the orbital angular momentum of the particle it is useful to relate it to another well-known quantity of the same dimension λ (Chakrabarti 1984, 1985; also see Abramowicz 1983 where λ was used for some co-ordinate transformation), defined as $\lambda^2 = 1/\Omega$, Ω being the angular velocity of the test particle ($= u^\phi/u^t$). In the present case one has,

$$\tilde{r}^2 = r^2 \Delta / (r-2)^2, \quad (6a)$$

$$\lambda^2 = r^2 \Delta / [(r-r_i)(r-r_\Omega)] = (r^3 + a^2 r - a l r_i) / (r-r_i). \quad (6b)$$

Notice that in both 2.² and the force components, the angular momentum of the particle appears in the combination ‘ all ’ or ‘ al ’, indicating the nature of the angular momentum coupling and the importance of the relative signs of the combination. Also, $r_\Omega = 2(1 - a\Omega)$. Among the most important properties of λ^2 , one notes that it *becomes equal to r^2 in the Schwarzschild geometry; the supremum (infimum) of its minima coincides with the last circular photon orbit for the prograde (retrograde) motion*, (Chakrabarti, 1985) and itself and its derivative diverge at the ‘ p^ϕ reversal radius’ $r = r_i$. Expressing the

force components explicitly in terms of p^ϕ one finds,

$$\begin{aligned} F_{cf} &= r^2 p^{\phi 2} [r(r-2)(r-3) - 2a^2] / [m(r-2)^4] \\ &= E^2 l^2 [r(r-2)(r-3) - 2a^2] (r-r_1)^2 / [r(r-2)(r-r_-)(r-r_+)]^2, \end{aligned} \quad (7)$$

$$F_g = -m/r^2 (1 - 2/r)^{-1}, \quad (8)$$

$$\begin{aligned} F_{co} &= 2aErp^\phi / [m(r-2)^3] \\ &= 2alE^2(r-r_1) / [r^2(r-2)^2(r-r_-)(r-r_+)]. \end{aligned} \quad (9)$$

Since the gravitational force F_g is independent of the angular momentum of the particle, we shall be primarily concerned with the centrifugal force F_{cf} and the Coriolis force F_{co} . Here r_- and r_+ denote the inner and the outer event horizons respectively. Notice that both the centrifugal and the Coriolis forces are zero everywhere on the ‘ p^ϕ reversal radius’ $r = r_l$ except when $r_l = r_-$, i.e., $2a/l = r_+$ and $r_l = r_+$, i.e., $2a/l = r_-$. Otherwise on the event horizons both the force components diverge. They also diverge on the ergosurface. In addition, the centrifugal force vanishes at $r = r_\infty$ where $r_\infty(r_\infty - 2)(r_\infty - 3) = 2a^2$. [The reason for calling these locations r is that the geodesic curvature $\mathcal{R} \propto r$ at these points (AP)].

To illustrate how the forces behave we draw in Figs 13 F_{cf} , F_{co} , and $F_{sum} = F_{cf} + F_{co}$ respectively for the test particles with $a/l = -0.3$ and 0.3 shown in dashed and solid curves respectively. The Kerr parameter a was chosen to be 0.95 throughout. One notes that for both the values, $a/l = \pm 0.3$, F_{cf} changes sign (Fig. 1a) at $0 < r_\infty < r_-$, at $r_- < r_\infty < r_+$, and also at $r_\infty > 2$. It also vanishes without changing sign at $r = r_l (= 1.4$ for $a/l=0.3$, 2.6 for $a/l = -0.3)$. Fig. 1b shows in detail the region outside the ergosphere and particularly the locations of r_∞ and r_l . F_{cf} diverges at $r = 0$, $r = r_\pm$ and $r = 2$. The Coriolis force F_{co} changes sign (Fig. 2) at $r=r_\pm$, $r = r_l$. The sum of these two angular momentum-dependent forces F_{sum} similarly reverses sign at several different places (Fig. 3). At the points where F_{sum} changes sign, only force acting on the particle is due to gravity, albeit the presence of rotation. To show the behaviour of F_{sum} over a large range of a/l ratio, the contours of $F_{sum} = 0$ are plotted in the ‘ $r-a/l$ ’ plane in Fig. 4a. One notices that among other things, $F_{sum} = 0$ on the straight line $r = 2(1 - a/l)$, except at $2a/l = r_\pm$.

Consider now a fluid configuration (say, an accretion disc surrounding the Kerr hole or a compact rotating object such as a neutron star) in hydrostatic equilibrium which constitutes a collection of such test particles. The stability of this configuration is determined by the condition

$$F(l, r) + G(r) = 0. \quad (10)$$

Here, $F(l, r)$ contains the forces which explicitly depend upon the angular momentum of the particle and $G(r)$ denote all the forces including gravity, which are independent of the angular momentum of the particle. When some test matter of angular momentum $l_0 = l(r_0)$ is displaced from its original position r_0 to a new position $r_0 + \delta r$, where the angular momentum of the matter is $l_0 + \delta l$, the perturbation of the total force is

$$\delta T = [F(l_1, r_1) + G(r_1)] - [F(l_0, r_1) + G(r_1)] = - \frac{\partial F}{\partial l} \frac{\partial l}{\partial r} \delta r. \quad (11)$$

Since in the stable situation, the displaced matter must come back to its original

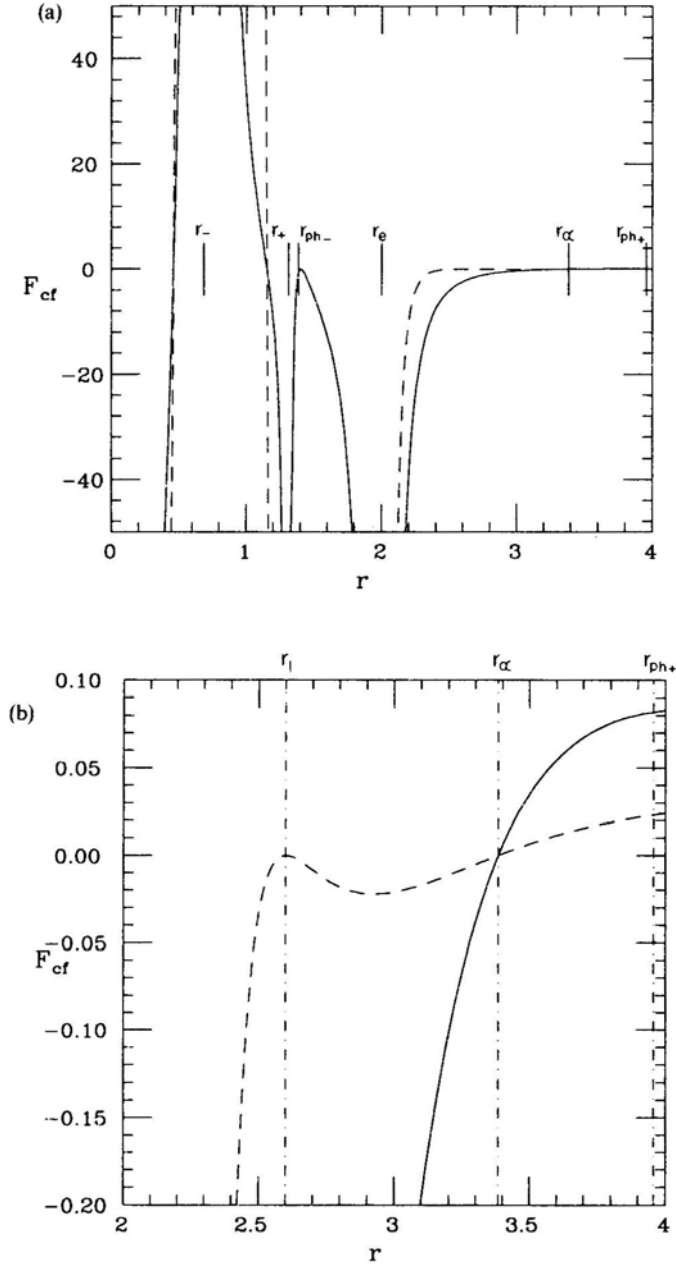


Figure 1. (a) The variation of the centrifugal force F_{cf} as a function of the radial distance on the equatorial plane in the Kerr geometry with angular momentum parameter $a = 0.95$. The solid curve is for $a/l = -0.3$ and the dashed curve is for $a/l = 0.3$. Various geometrical important locations are indicated by the vertical solid lines. They are from the left to the right r_- , the inner horizon, r_+ , the outer horizon, r_{ph-} , the inner photon orbit, r_e , the ergosphere and r_{ph+} , the outer photon orbit. Also shown is r_∞ outside the horizon where the geodesic curvature \mathcal{R} diverge. (b) An expanded view of the region outside the ergosphere of (a). In addition to r_∞ where F_{cf} vanishes independent of the angular momentum of the particle, we show the ‘ p^ϕ reversal radius’ r_l .

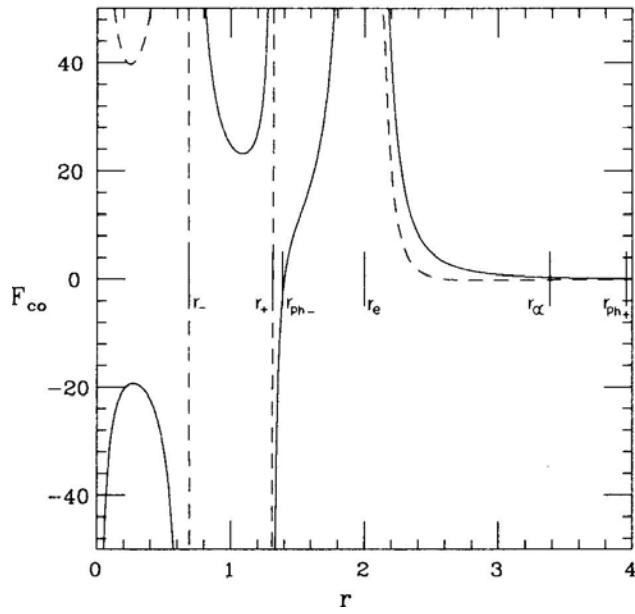


Figure 2. A figure similar to Fig. 1a showing the variation of the *Coriolis* force F_{co} .

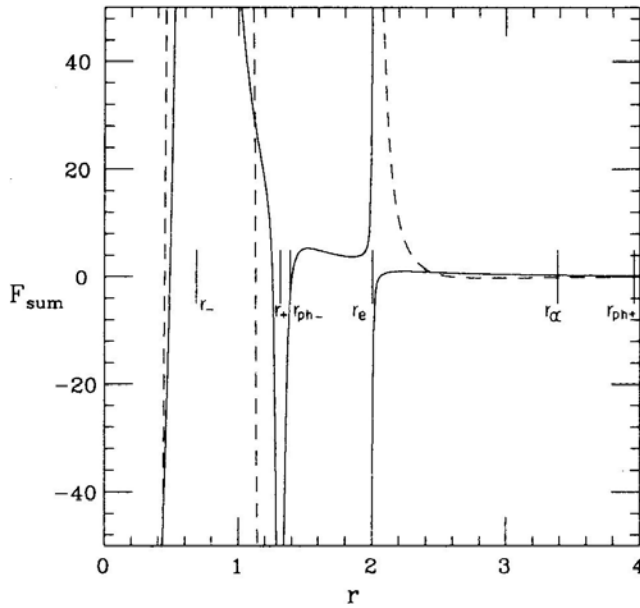


Figure 3. A figure similar to Fig. 1a showing the variation of the *total* angular-momentum-dependent force F_{sum} acting on the test particle.

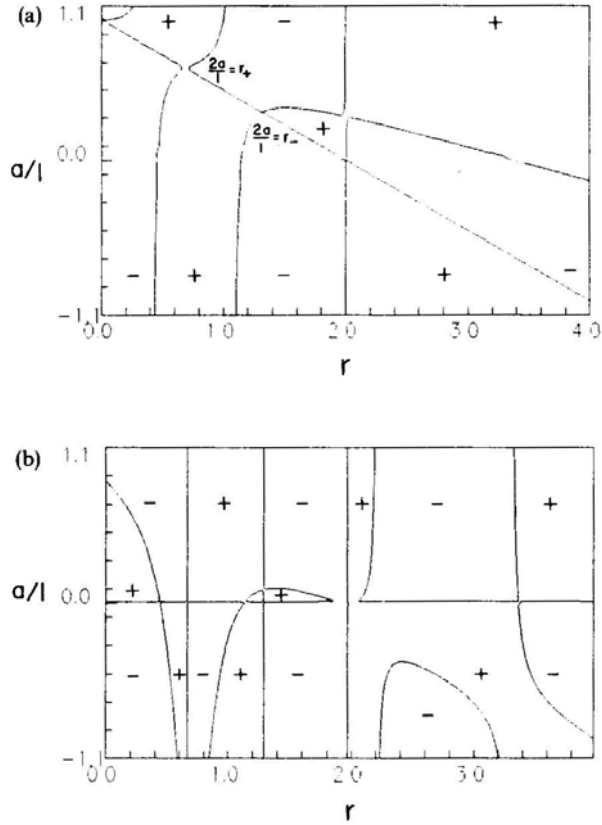


Figure 4. (a) The contours of $F_{\text{sum}} = 0$ are shown in the ' r - a/l ' plane. The signs + and - indicate the outward and the inward directed force respectively. Notice that the F_{sum} vanishes everywhere on the $r = r_l$ line (the so-called ' p^ϕ reversal radius') except where $2a/l = r_\pm$. (b) The contours of $\partial F_{\text{sum}} / \partial l = 0$ separating the regions where the Rayleigh criterion for stability of a rotating configuration reverses sign. The signs + and - indicate the signs of $\partial l / \partial r$ which are required for the configuration to be stable under axisymmetric perturbation.

Position, $\partial T / \partial r < 0$, i.e.,

$$\frac{\partial F}{\partial l} \frac{\partial l}{\partial r} > 0.$$

In the present situation, $F(l, r) = F_{\text{sum}}$. The gradient $\partial F_{\text{sum}} / \partial l$ need not be positive everywhere as in the Newtonian case. Indeed, this quantity reverses its sign several times inside as well as outside the horizon. Fig. 4b shows its behaviour for a large range of a/l ratio. Only the contours of $\partial F_{\text{sum}} / \partial l = 0$ are shown and the sign of the gradient $\partial l / \partial r$ which keeps the equilibrium configuration stable are noted. The important conclusion of this exercise is that the familiar Rayleigh criterion of stability, namely, $\partial l / \partial r > 0$ does not hold everywhere in the Kerr geometry.

The importance of the reversals of the gradient of the angular momentum distribution could be significant, particularly, in the study of the structure of the compact stars and the geometrically thick accretion discs. In these cases the complete solution has to be obtained fully self-consistently by solving Einstein's equations in the

presence of the gravitating matter. The fact that F_{sum} points *inwards* in some region may be the cause of the observation of Chandrasekhar & Miller (1974) who show that in the context of general relativity, the ellipticity of a rotating homogeneous Maclaurin spheroid first increases and then decreases in the course of its collapse if the total angular momentum and the mass are kept fixed. Equivalently, if a compact star accretes mass and angular momentum (as is believed to be the case for the millisecond pulsars), it is not necessary that the star becomes progressively unstable, since addition of angular momentum does not always imply enhancement of centrifugal force. In fact the star may pass through some stable phase beyond the well-known marginal configuration in which the angular velocity at the outer surface is equal to the Keplerian velocity. A complete study is essential to settle this important issue. Our result, presented here at the test particle level, can only give guidance as to what to expect. Recently, Abramowicz & Miller (1989) consider this aspect, and show that the Chandrasekhar and Miller result for slowly rotating bodies may be explained within the framework of the general discussion of rotational effects in a strong gravitational field as given by AP.

References

- Abramowicz, M. A. 1983, *Astrophys. J.*, **254**, 784.
Abramowicz, M. A., Carter, B., Lasota, J. P. 1988, *Gen. Rel. Grav.*, **8**, 1173.
Abramowicz, M. A., Prasanna, A. R. 1989, *Mon. Not. R. Astron. Soc.*, (to appear) (AP).
Abramowicz, M. A., Miller, J, 1989, *Mon. Not. R. Astr. Soc.*, (to appear).
Chakrabarti, S. K. 1984, *Active Galactic Nuclei*, Ed. J. E. Dyson, Manchester Univ. Press.
Chakrabarti, S. K. 1985, *Astrophys. J.*, **288**, 1.
Chandrasekhar, S., Miller, J. C. 1974, *Mon. Not. R. Astr. Soc.*, **167**, 63.